International Journal of Mass Spectrometry 300 (2011) 65–69

Contents lists available at ScienceDirect

International Journal of Mass Spectrometry

journal homepage: www.elsevier.com/locate/ijms

Short communication

Accurate in situ calibration of the energy bandwidth and the zero-energy offset in SIMS analysis using magnetic sector field instruments

Klaus Wittmaack*

Helmholtz Zentrum München, Institute of Radiation Protection, Geb. 36, D-85758 Neuherberg, Germany

ARTICLE INFO

Article history:
Received 24 November 2010
Received in revised form
13 December 2010
Accepted 14 December 2010
Available online 21 December 2010

Keywords:
Secondary ion mass spectrometry
Energy bandwidth
Energy offset
Gas-phase ionization

ABSTRACT

Instruments used for basic studies in secondary ion mass spectrometry (SIMS) are usually not very well characterized in terms of important experimental parameters like the energy bandwidth and the origin of the energy scale. A proof-of-concept is presented which shows that in magnetic sector field mass spectrometers this kind of information can be obtained rather easily by determining the spectral features of ions generated by primary ion impact on a gas deliberately introduced in the extraction region above the sample. Owing to the negligible kinetic energy of the gas atoms, the measured energy spectrum exhibits a well-defined edge which corresponds to moving the energy bandpass through the gas–solid interface at the target surface. The energy resolution function can be derived as the derivative of the measured data. For high accuracy it is mandatory that the detected ions originate from a volume that is uniformly illuminated by the primary ion beam. The validity of the concept is demonstrated by evaluating recently published literature data. Even though the experiments were performed with a rather large bandwidth, shown to be 30.2 eV, the highly symmetric resolution function allowed the origin of the energy scale to be determined with an accuracy of ±0.2 eV. The potential of the approach needs to be explored in more detail by varying the relevant experimental parameters.

1. Introduction

Interpretation of experimental data on secondary ion emission is often significantly hampered by the fact that the energy of ejected ions, E, and the bandwidth, ΔE, of the employed energy analyzer are not known sufficiently well. Energy spectra of secondary ions are commonly recorded by varying the bias potential, V_t, of the target while keeping the voltages applied to the energy analyzer fixed. This is an established technique, irrespective of whether magnetic sector fields [1] or quadrupole filters are used for mass analysis [2]. Target-bias to energy conversion involves the simple relation [3].

$$E = q\,e\,\left(V_t^0 - V_t\right), \tag{1}$$

where q is the charge state of the ion and e the elementary charge. The accuracy with which E can be determined rests on a knowledge of $V_t^0 = V_t(E = 0)$, the target bias corresponding to the origin of the energy scale, $E = 0$. A generally accepted procedure for determining V_t^0 does not exist. Attempts have been made to calibrate the energy analyzer of the employed SIMS instrument by using a beam of alkali ions emitted from a heated surface with thermal energies (<0.1 eV) [4–6], but this approach suffers from unknown contact potential differences [7].

In view of these difficulties, recent studies on Cs^+ secondary ion energy spectra observed during Cs implantation [8] or at increasing rates of Cs vapour deposition [9] were restricted to determining the spectral shifts associated with changes in the sample's work function. The experiments were performed using magnetic sector field instruments, either a Cameca IMS 4f [8] or a modified version thereof [9], the so-called Cation Mass Spectrometer [10]. The normalized Cs^+ spectra [8,9] exhibited surprisingly steep low-energy edges, rising from 16% to 84% of the peak level within less than 1 eV. This observation is strongly at variance with a quoted energy bandwidth ΔE of 2–3 eV, a number presumably specified by the manufacturer for a very narrow width of the energy defining slits. Actual measurements of ΔE have not been cited, but are urgently needed.

The purpose of this communication is to present the proof-of concept for the idea that ΔE and V_t^0 may be determined in magnetic sector field instruments, in situ and with high accuracy, by making use of spectral features observed when ions are produced in a gas deliberately introduced in the space between the target and the extraction electrode.

2. Data basis

The results presented below are based on an evaluation of data recently reported by Desgranges and Pasquet (D&P) [11]. The study, performed with a Cameca IMS 6f, primarily aimed at presenting an

* Tel.: +49 89 3187 2439; fax: +49 89 3187 2942.
E-mail address: wittmaack@helmholtz-muenchen.de

1387-3806/$ – see front matter © 2010 Elsevier B.V. All rights reserved.
doi:10.1016/j.ijms.2010.12.009

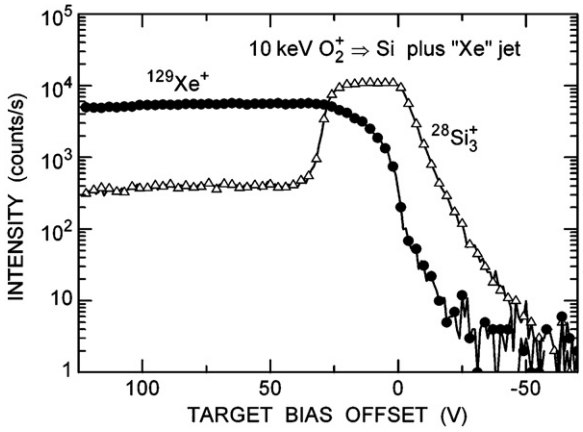

Fig. 1. Raw energy spectra of gas and target specific ions generated during 10 keV O_2^+ bombardment of a silicon sample immersed in a gas containing xenon. The energy of the detected ions increases from left to right. The original data and the labels assigned to the analyzed secondary ion are due to Desgranges and Pasquet [11].

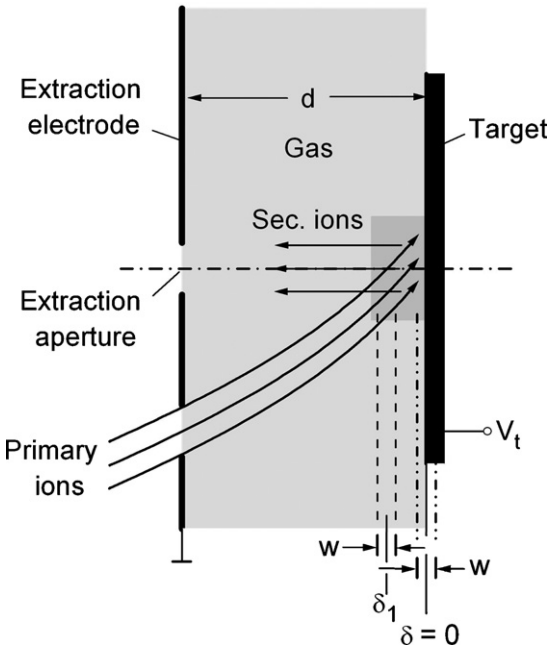

Fig. 2. Schematic illustration of the experimental geometry in the vicinity of the target.

improved detection sensitivity for SIMS analysis of Xe in UO_2 using 10 keV O_2^+ bombardment in combination with simultaneous exposure of the sample to a jet of oxygen gas. Some of the problems encountered in the data interpretation were discussed recently [12]. As a side aspect, D&P also explored the formation of Xe^+ ions generated by O_2^+ impact on gaseous xenon. The gas was fed into the volume above the sample, through the same capillary that usually serves to shape and position the oxygen jet [11]. In that particular experiment the target was made of silicon. The high efficiency of ion induced gas analysis was demonstrated some time ago for 5 keV Ar^+ and N_2^+ impact on Ar and residual gases in a quadrupole based SIMS instrument [13]. To avoid interference with secondary ions emitted from the sample, the beam was passed through a hole in the target holder.

Inspection of the results of D&P (Fig. 1 in Ref. [11]) suggested that the data might serve well for extracting the energy bandwidth as well as the absolute position of its centre, equivalent to V_t^0. On request, the raw data of that study were kindly made available by one of the authors [14]. Different from the linear scale used in the original data publication [11], the results reproduced in Fig. 1 are presented on a logarithmic intensity scale. The spectra were recorded in steps of 1 V by varying the offset ΔV_t, superimposed on the fixed target bias of 5 kV. D&P estimated ΔV_t^0 to be 15 V [11]. Presumably with the aim of achieving high signals, the measurements were carried out with a comparatively wide bandwidth ΔE, quoted as approximately 25 eV [11]. As a result, the energy spectrum of Si_3^+ ions emitted from the silicon target exhibits a very broad peak, much broader than the distribution previously measured with a resolution of about 1 eV [15]. The high-energy tail of the Si_3^+ spectrum in Fig. 1, on the other hand, is fairly similar to the previously observed tail [15] (the secondary ion energy increases from left to right).

At high target bias, i.e., for $V_t > 40$ V, the spectrum assigned to Si_3^+ exhibits an unusual plateau. A comparison with the spectrum of $^{129}Xe^+$ suggested that the signals observed at m/z 84 could be due to $^{84}Kr^+$, indicating the presence of krypton as an impurity in the xenon jet. On inquiry, the contacted authors [14] specified the composition of the supply gas as 75.6% helium, 18.4% xenon and 6.04% krypton, thus confirming the 'impurity' conjecture. Accounting for the natural abundance of ^{129}Xe (26.4%) and ^{84}Kr (57%), the concentration of these isotopes in the supply gas was 4.86% and 3.44%, respectively. Additionally provided information [14] included the beam current (15 nA) and the raster scanned area (250 μm × 250 μm).

3. Detailed concept and data evaluation

To ease discussion, the relevant section of the experimental arrangement is sketched in Fig. 2. The O_2^+ beam, initially at 15 keV, entered the secondary ion extraction field through a hole in the grounded extraction electrode. Owing to the oblique incidence of the beam and the high target bias of 5 kV, the primary ions were deflected significantly, arriving at the target at 10 keV. The incident ions caused secondary ion emission from the solid sample as well as ionization of the gas fed into the space between the target and the extraction electrode (spacing $d = 5$ mm, field strength $F_a = 1$ V/μm). Depending on the distance δ from the target at which ionization of gas atoms took place, the generated gas ions did not experience the full extraction voltage of 5 kV but only the fraction $(1 - \delta/d)$. Since the thermal energy of the gas atoms (~0.025 eV) was negligible, the accelerated gas ions (assumed to be singly charged) appeared in the energy spectrum at a 'negative' energy $E = -\delta e F_a$. With an energy bandwidth $\Delta E = weF_a$, the detected ions originated from distances between $\delta - w/2$ and $\delta + w/2$, see Fig. 2.

Clearly, an interpretation of the gas-phase ionization data will be straightforward only if the ion density in the inspected volume was constant. As Fig. 3 shows, this requirement was fulfilled in the experiment of D&P over a distance of at least 50 μm, i.e., for V_t between about 30 and 80 V, and for Xe^+ as well as for Kr^+. The dash-dotted and dashed lines represent the results of linear regression analyses, applied to the data represented by solid symbols. The slopes are negligible (<0.5 counts/s per volt), i.e., within statistical uncertainty the intensities were independent of ΔV_t. The measured $^{129}Xe^+/^{84}Kr^+$ intensity ratio was 14, the corresponding ratio of the gas concentrations 1.4. Hence the efficiency of ionizing Kr was 10% compared to Xe. Charge transfer ionization of Xe by O_2 (ionization potential $I_{Xe} = 12.13$ eV, $I_{O_2} = 12.07$ eV [16]) is almost resonant. By contrast, ionization of Kr ($I_{Kr} = 14.00$ eV) by O_2^+ is far off resonance and the potential energy provided by the primary ion is too low by

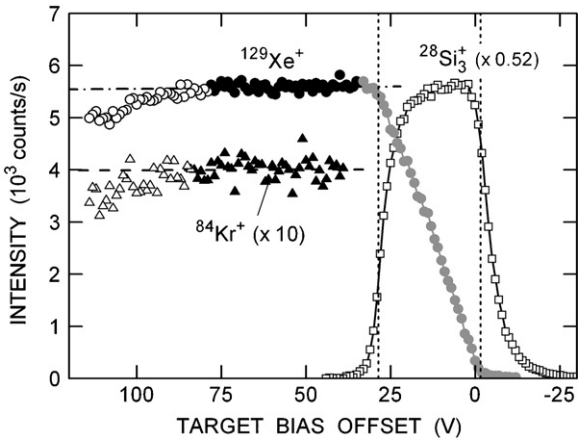

Fig. 3. Details of the spectra in Fig. 1. The signals recorded at m/z 84 are now separated into contributions due to Kr^+ and Si_3^+. The full black symbols denote the region where the intensity due to gas ions was constant within experimental accuracy (dash-dotted and dashed lines). The vertical short-dashed lines mark the half width of the derived resolution function (see Figs. 4 and 5).

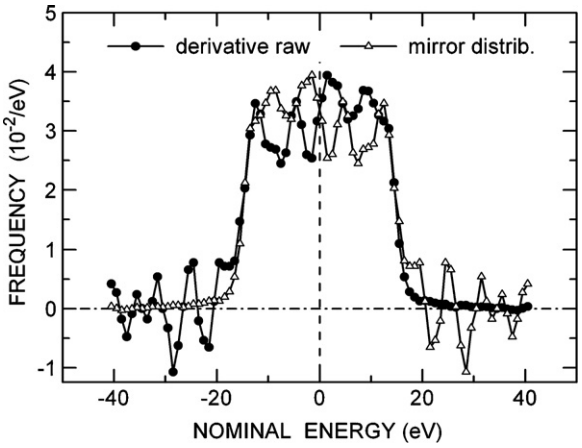

Fig. 4. Resolution function $R(E)$ derived as the derivative of the smoothed Xe^+ data (solid circles) and the mirror image of $R(E)$ (open triangles). The mirror plane is the origin of the energy scale, $E = 0$.

almost 2 eV. Therefore, an ionization efficiency of 10% for Kr relative to Xe must be considered very high, being hard to explain in standard charge-transfer terms, unless we assume that a sizable fraction of the incident O_2^+ ions was in a excited state. Undoubtedly, the finer details of non-resonant ion-impact ionization need to be explored in more detail.

Returning to Fig. 3 we note that, for $\Delta V_t > 80$ eV, the Xe^+ and Kr^+ signals started to decrease, slowly first and then more rapidly. This observation suggests that, owing to the small size of the focussed beam (presumably < 20 μm) and the oblique angle of incidence, the gas present at distances $\delta > 60$ μm, in a narrow volume around the surface normal through the centre of the extraction aperture, was not fully intersected by the incident beam (see Fig. 2).

As the target bias was reduced below about 30 V, the analyzed layer of thickness w started to pass through the sample surface. Consequently, the number of Xe^+ ions contained in the energy window ΔE decreased as well. Provided the entrance slit of the energy analyzer was hit by a uniform current density of secondary ions, one would have expected the signal to decrease linearly with decreasing target bias. The results obtained by D&P are largely in accordance with expectation (see grey solid circles in Fig. 3). A closer inspection of the data reveals a marginal change in slope near half-height, possibly indicating that the entrance slit of the energy analyzer was not filled in an exactly uniform manner.

On the basis of the presented concept, the variation of the Xe^+ intensity, measured in passing the energy window through the sample surface, constitutes the convolution of the energy-resolution function with a sharp edge, the surface. One may also view this procedure as a step-wise integration over the resolution function. Hence, the derivative of the measured intensity is the resolution function itself, $R(e\Delta V_t^0)$ or $R(E)$. Prior to determining the derivative, the statistical uncertainty of the Xe^+ data, notably in the plateau region, was reduced somewhat by passing them through a three-point smooth (standard deviation of the raw data in the plateau region 78 counts/s, close to the square root of the mean signal, 74.8 counts/s; smoothed data: standard deviation 42 counts/s). Smoothing is justified because the derivative of the plateau data determines the scatter of the resolution function in a region where its mean is zero.

The resolution function $R(E)$ derived from the smoothed Xe^+ data is shown in Fig. 4 as solid circles. For subsequent use in a convolution exercise, the data are normalized to an integral of unity. Very remarkable is the observation that $R(E)$ exhibits very steep and symmetrical edges, confirmed by superimposing the mirror image $R_{mr}(E)$ (open triangles in Fig. 4) on $R(E)$. The symmetry implies that the centre of $R(E)$, equivalent to $E = 0$, can be determined rather safely. The result is $\Delta V_t^0 = 13.5 \pm 0.2$ V, 1.5 V lower than the estimate of D&P [11]. The uncertainty of 0.2 V was derived by deliberately shifting $R_{mr}(E)$ and comparing the deviation from $R(E)$ at the sharp edges.

The statistical uncertainty in the central region of $R(E)$ and in the left hand tail (constituting the derivative in the plateau region of the Xe^+ spectrum) is not fully satisfactory. In future experiments this deficiency could be removed by tuning the experimental parameters (beam current, gas pressure, counting time) for better counting statistics. Nevertheless, as shown below, $R(E)$ can be used as such to perform very meaningful convolution tests. This is due to the fact that convolution involves smoothing. Irrespective of this advantageous feature, it appeared desirable to assess relevant features of $R(E)$ in more detail, making optimum use of the available data. The open circles in Fig. 5 show $R^*(E)$, calculated in the central region as $(R(E) + R_{mr}(E))/2$. The tails on either side were assumed to be the same as on the right-hand side of $R(E)$, the argument being that this side is not suffering from the statistical uncertainties encountered in the plateau region. For comparison, the thick solid line shows a

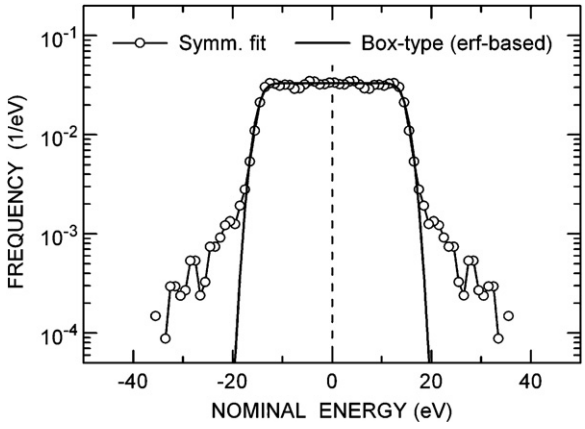

Fig. 5. Optimized resolution function derived by taking the mean of the data of Fig. 4 in the central section and by using only the statistically most meaningful data for tail definition. The thick solid line is the idealized resolution function according to Eq. (2).

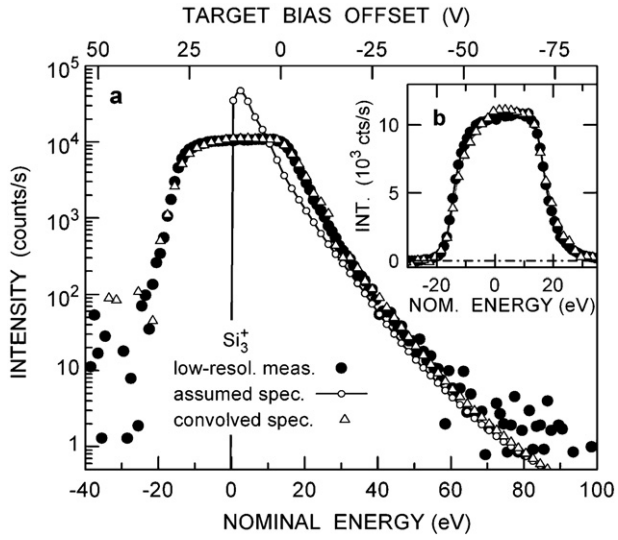

Fig. 6. Comparison of the measured Si_3^+ spectrum (solid circles) with the spectrum obtained by convolving the high-resolution Si_3^+ reference spectrum (open circles) with the resolution function of Fig. 4; (a) logarithmic, (b) linear intensity scale.

normalized box-shaped resolution function of the form

$$R_b(E) = \frac{1}{4\Delta E}\left[1 + \mathrm{erf}\left(\frac{E + 0.5\Delta E}{2^{0.5}\sigma_E}\right)\right]\left[1 - \mathrm{erf}\left(\frac{E - 0.5\Delta E}{2^{0.5}\sigma_E}\right)\right] \quad (2)$$

Eq. (2) constitutes the convolution of a rectangular box with a Gaussian of standard deviation σ_E. An optimum fit to the experimental data down to about 10% of the plateau level (frequency 3×10^{-3}/eV) was achieved with $\Delta E = 30.2 \pm 0.5$ eV and $\sigma_E = 1.6$ eV.

The deviations of $R^*(E)$ from $R_b(E)$ evident in Fig. 5 in the extended tails may be attributed to Xe^+ ions scattered off other gas atoms in the extraction field with a cross section roughly determined by the size of the atoms. Owing to the tight geometry, the gas pressure generated by the jet in front of the target may have been a factor of 10–20 higher than at a remote location where the pressure gauge was located. The quoted pressure reading of 5×10^{-6} mbar [11] thus converts to a near-surface pressure of up to 10^{-4} mbar. With a gas density N, a scattering cross section $\sigma = (\pi/4)D^2$ for atoms of diameter D, and a distance L traversed by an ion in the gas, the probability P for scattering can be estimated as $N\sigma L = (\pi/4)D^2NL$. With $D_{Xe} = 4.37 \times 10^{-8}$ cm, $N(10^{-4}\ \mathrm{mbar}) = 2.6 \times 10^{-12}\ \mathrm{cm}^{-3}$ and $L = d = 0.5$ cm we have $P = 2 \times 10^{-3}$, which is the right order of magnitude (in a dedicated study one should make sure that the signal recorded at m/z 129 does not contain any noticeable contribution due to molecular secondary ions sputtered from the Si target, e.g. $(^{28}Si)_3(^{29}Si)^{16}O^+$).

In a first test, the validity of the derived resolution function was explored by means of a simple convolution test. The Si_3^+ spectrum of D&P, shown in Fig. 6 as solid circles, was obtained by subtracting the Xe^+ spectrum, normalized to the height of the Kr^+ spectrum in the plateau region of Fig. 1, from the spectrum measured at m/z 84. A high-resolution Si_3^+ reference spectrum with the same integral yield, represented in Fig. 6(a) by small open circles, was constructed on the basis of previously reported data [15] as the sum of seven Gaussian distributions, centred at increasing energies (ranging from 2 to 55 eV), with increasing standard deviation (2–22 eV) and decreasing peak height. This spectrum was convolved with $R(E)$ to obtain the calculated Si_3^+ spectrum shown in Fig. 6 by open triangles. The agreement between the measured and the convolved spectrum is seen to be quite good, both on a logarithmic and a linear intensity scale, see panels (a) and (b) of Fig. 6. It must be noted, however, that in order to obtain almost perfect overlap of the two spectra, the convolved spectrum had to be shifted by 2 eV towards lower energies. This shift was exactly the same as the peak position of the first (and dominant) Gaussian distribution of the composite Si_3^+ reference spectrum. It is easy to show that a narrow high-intensity feature at the leading edge of an extended distribution dominates the front-end shift obtained by convolution with a (very) broad resolution function. Since the described convolution exercise was not meant to produce ultimate agreement by artificially constructing best-fit input parameters, the assumed Si_3^+ reference spectrum was not refined. Given the availability of only one set of experimental data, it was not possible, at this point, to go beyond demonstrating the proof-of-concept.

4. Conclusion and perspectives

It has been shown that the origin of the energy scale of secondary ions and the energy resolution of a standard magnetic sector field SIMS instrument can be determined rather easily by an approach that makes use of gas phase ionization in the volume immediately above the sample. The method has several advantages. (i) All necessary hardware is already available on most if not all of the Cameca IMS 3f to 6f instruments currently in use in a large number of laboratories worldwide. The calibration procedure can be used (ii) in combination with the actual sample under study or with a test sample of the same material, (iii) for any setting (width) of the energy slits, and (iv) with essentially free choice of the gas, the primary ion species and the beam current. Nevertheless it would be desirable to explore the finer features of the method in more detail than in the experiment of D&P which was not designed for the purpose of interest here.

More dedicated future studies should address the following aspects: (I) effect of beam current, beam size and scan width, including static beams (no raster scan). One purpose would be to maximize the count rate for good statistical accuracy (note that the beam current used by D&P [11] was quite low, only 15 nA). It will also be important to explore the size and position of the volume in front of the target that is best suited for calibration purposes. For an optimum comparison with the energy spectra of secondary ions, it appears desirable to place the beam exactly on axis of the extraction aperture. (II) The gas mixture used by D&P was chosen in the context of their work on SIMS analysis of irradiated nuclear fuels. To optimize gas pressure in terms of counting statistics and, at the same time, minimize scattering of generated ions at atoms of the bleed-in gas, it will be desirable to use pure gases. (III) Of great interest would be studies in which the width of the energy defining slits is varied in a systematic manner. The resolution functions derived from such measurements should feature the same sharpness of the edges, differing only in width. Using secondary ions with narrow energy distributions, like cluster ions, one could test convolution issues in situ, directly comparing spectra measured with narrow and wide bandwidth. (IV) In very dedicated experiments it might also be worth exploring whether or to what extent work function changes of the target, produced by Cs implantation, might have an effect on the position the energy distribution of ionized gases.

Acknowledgement

I thank Bertrand Pasquet for kindly providing the raw data evaluated in this study as well as for additional information on relevant experimental details.

References

[1] G. Blaise, G. Slodzian, Rev. Phys. Appl. 8 (1973) 105.
[2] K. Wittmaack, Surf. Sci. 53 (1975) 626.
[3] K. Wittmaack, Int. J. Mass Spectrom. Ion Phys. 269 (2008) 24.
[4] P.H. Dawson, P.A. Redhead, Rev. Sci. Instrum. 48 (1977) 159.
[5] J.H. Craig Jr., J.L. Hock, J. Vac Sci. Technol. 17 (1980) 1360.

[6] M.L. Yu, Phys. Rev. Lett. 47 (1981) 1325.
[7] K. Wittmaack, Vacuum 32 (1982) 65.
[8] H. Gnaser, Phys. Rev. B 54 (1996) 17141.
[9] T. Wirtz, H.-N. Migeon, Surf. Sci. 561 (2004) 200.
[10] T. Wirtz, B. Duez, H.-N. Migeon, H. Scherrer, Int. J. Mass Spectrom. 209 (2001) 57.
[11] L. Desgranges, B. Pasquet, Nucl. Instrum. Methods Phys. Res. B 215 (2004) 545.
[12] K. Wittmaack, Nucl. Instrum. Methods Phys. Res. B 266 (2008) 5151.
[13] K. Wittmaack, Int. J. Mass Spectrom. Ion Phys. 42 (1982) 43.
[14] B. Pasquet, Personal Communication, 2010.
[15] K. Wittmaack, Phys. Lett. A 69 (1979) 322.
[16] D.R. Lide (Ed.), CRC Handbook of Chemistry and Physics, Taylor & Francis, Boca Raton, 2005.